文章编号:2095-6134(2017)03-0289-07

Influence of Zeeman magnetic field on the nodal structure of unconventional superconductors*

CHEN Chongju, JIN Biao†

(*School of Physical Sciences*, *University of Chinese Academy of Sciences*, *Beijing* 100049, *China*)

(Received 3 May 2016; Revised 13 May 2016)

Chen C J, Jin B. Influence of Zeeman magnetic field on the nodal structure of unconventional superconductors[J]. Journal of University of Chinese Academy of Sciences, 2017,34(3):289-295.

Abstract In most of the unconventional superconductors, the quasiparticle excitation spectrum possesses line or point nodes leading to a power-law temperature dependence in the thermodynamic quantities and transport coefficients at low temperatures. In this work we show analytically that an applied weak Zeeman magnetic field can drastically alter these nodal structures. In particular, we predict that surface nodes might be induced on the Fermi surface under certain circumstances. Our numerical calculations of electronic specific heat for selected spin-singlet and spin-triplet states confirm that the change in the nodal structure may accompany significant modification in the power-law temperature dependence.

Keywords superconductivity; nodal structure; Zeeman field; specific heat

CLC number: O469 **Document code**: A **doi**: 10.7523/j.issn.2095-6134.2017.03.003

Zeeman 磁场对有节点非常规超导体节点结构的影响

陈崇巨,金 彪

(中国科学院大学物理科学学院, 北京 100049)

摘 要 在大部分非常规超导体中,准粒子激发谱中存在着"线节点"或"点节点"。这些节点的存在,导致热力学量和输运系数在低温区的温度变化呈现幂次律。解析分析表明,外加的弱 Zeeman 磁场会显著影响节点的结构。尤其是,预言在某些情况下 Zeeman 磁场可能在费米面上诱导出"面节点"。计算若干自旋单态和自旋三重态的电子比热,结果显示外加的弱 Zeeman 磁场对节点结构的影响会导致幂次律产生巨大变化。

关键词 超导; 节点结构; Zeeman 磁场; 电子比热

Over the past three decades, unconventional superconductivity with gap symmetry other than s-wave has been found in several classes of materials, including the heavy-Fermion superconductors with or without the spatial inversion symmetry, the high-T_c superconductors, and the organic superconductors[1-2].

* Supported by Science Research Fund of UCAS (Y25102BN00)

†Corresponding author, E-mail: biaojin@ucas.ac.cn

The study of exotic properties of unconventional superconductors has become a central issue in the field of condensed matter physics. Most of unconventional superconductors have nodes (zeros) in the gap functions along certain directions in the momentum space. Since the nodal structure is intimately related to the pairing interaction, its identification is of fundamental importance. The anisotropic nodal structure in unconventional superconductors has mainly been investigated by probing the thermally excited quasiparticles. Experimentally, the temperature dependence of several thermodynamic quantities and transport coefficients such as electronic specific heat $C_e(T)$, nuclear magnetic resonance relaxation rate $T_1^{-1}(T)$, London penetration depth $\lambda(T)$, and thermal conductivity $\kappa(T)$ have been extensively used so far to explore the nodal topology of unconventional superconductors.

For a superconductor with the order parameter belonging to a one-dimensional representation of a given crystal symmetry, the nodal topology is restricted to either line nodes or point nodes. The existence of Bogolubov quasiparticle excitations in the neighborhood of these nodes gives rise to a non-BCS behaviour in the temperature dependence of thermodynamic quantities and transport coefficients, particularly at low temperatures where the contributions from the nodes are dominant. In the clean limit, the thermodynamic quantities and transport coefficients exhibit a power-law $\sim T^n$ temperature dependence as $T \to 0$, other than an exponential temperature dependence $\exp(-\Delta_0/T)$ as in the case of the fully gapped s-wave superconductor. According to the generalized BCS theory, the power-laws in temperature depend on only the dimension of the structures of gap nodes (i. e., points or lines) and the rate at which the gap vanishes in the neighborhood of the nodes. In the case of electronic specific heat $C_e(T)$, one has $n = 3$ for point nodes with linearly varying gap amplitude around the nodal point, and $n = 2$ for line nodes as well as point nodes where the gap is quadratic in distance from the nodal point in the momentum space[3-4].

However, the hint in the nodal structure might be hidden by some extrinsic origins of low-lying states within energy gap. Impurities are at the forefront of the extrinsic origin. Scattering by a sufficiently small amount of impurities in unconventional superconductors may cause decrease in the critical temperature and bring in changes in the nodal structure leading to the power-law dependence ineffective. This issue is discussed extensively within and beyond the Born approximation[5-8]. Another extrinsic origin leading to similar effects might be an applied weak Zeeman magnetic field (ZF) which breaks the time-reversal symmetry. Recently the role of a weak ZF in the noncentrosymmetric superconductors[2], where the Cooper pair state is a mixture of spin-singlet and spin-triplet states, has been discussed by several authors[9-11]. The stability of the suggested accidental line nodes[12-13] and the possible types of nodal structures induced by ZF have been the focuses of discussion[9,14]. In this work, we investigate how the nodal structure in pure nodal spin-singlet and spin-triplet states as well as the power-law temperature dependence for electronic specific heat are affected by an applied weak ZF.

1 Formulation

Let us consider a superconductor modeled by the Bogoliubov-de Gennes Hamiltonian

$$H = H_0 + H_{\text{int}}. \tag{1}$$

The first term H_0 is for a noninteracting conduction electron system subjected to a ZF,

$$H_0 = \sum_{\boldsymbol{k}} \sum_{\alpha,\beta} (\epsilon_k \boldsymbol{\sigma}_0 + \boldsymbol{h} \cdot \boldsymbol{\sigma})_{\alpha\beta} c_{\boldsymbol{k}\alpha}^{\dagger} c_{\boldsymbol{k}\beta}, \tag{2}$$

where $c_{\boldsymbol{k}\alpha}^{\dagger}(c_{\boldsymbol{k}\alpha})$ creates (annihilates) an electron with wave vector $\boldsymbol{k} = k(\sin\theta_k\cos\phi_k,\ \sin\theta_k\sin\phi_k,\ \cos\theta_k)$ and spin α, $\boldsymbol{\sigma} = (\sigma_x, \sigma_y, \sigma_z)$ denotes the Pauli matrices, $\boldsymbol{\sigma}_0$ is the 2×2 unit matrix, ϵ_k is the parabolic bare band dispersion measured relative to the chemical potential μ and restricted to $|\epsilon_k| < \omega_c$ with ω_c being the usual cutoff energy. The ZF is specified by $\boldsymbol{h} = h(\sin\theta_h\cos\phi_h, \sin\theta_h\sin\phi_h, \cos\theta_h)$.

The second term in (1) describes the pairing interaction

$$H_{\mathrm{int}} = \frac{1}{2}\sum_{\boldsymbol{k}}\sum_{\alpha,\beta}[\Delta_{\boldsymbol{k},\alpha\beta}c^{\dagger}_{\boldsymbol{k}\alpha}c^{\dagger}_{-\boldsymbol{k}\beta} + \Delta^{\dagger}_{\boldsymbol{k},\alpha\beta}c_{-\boldsymbol{k}\alpha}c_{\boldsymbol{k}\beta} + \Delta_{\boldsymbol{k},\alpha\beta}F^{\dagger}_{\boldsymbol{k},\beta\alpha}], \quad (3)$$

with the anomalous averages $F_{\boldsymbol{k},\alpha\beta} = \langle c_{\boldsymbol{k}\alpha}c_{-\boldsymbol{k}\beta}\rangle$, and the gap function defined by

$$\Delta_{\boldsymbol{k},\alpha\beta} = -\sum_{\boldsymbol{k}'}\sum_{\lambda,\mu}V_{\beta\alpha,\lambda\mu}(\boldsymbol{k},\boldsymbol{k}')F_{\boldsymbol{k}',\lambda\mu}, \quad (4)$$

where $V_{\alpha\beta,\lambda\mu}(\boldsymbol{k},\boldsymbol{k}')$ denotes the pairing potential. The Pauli principle requires that $\Delta_{\boldsymbol{k},\alpha\beta} = -\Delta_{-\boldsymbol{k},\beta\alpha}$.

By using the Nambu vector operator, $\boldsymbol{\Psi}_{\boldsymbol{k}} = (c_{\boldsymbol{k}\uparrow}, c_{\boldsymbol{k}\downarrow}, c^{\dagger}_{-\boldsymbol{k}\uparrow}, c^{\dagger}_{-\boldsymbol{k}\downarrow})^{\mathrm{T}}$, where $(\cdots)^{\mathrm{T}}$ stands for the transposing operation, we can rewrite the Hamiltonian in a more compact form

$$H = \frac{1}{2}\sum_{\boldsymbol{k}}\boldsymbol{\Psi}^{\dagger}_{\boldsymbol{k}}\check{\boldsymbol{H}}_{\boldsymbol{k}}\boldsymbol{\Psi}_{\boldsymbol{k}} + \sum_{\boldsymbol{k}}\epsilon_k + \frac{1}{2}\sum_{\boldsymbol{k}}\sum_{\alpha,\beta}\Delta_{\boldsymbol{k},\alpha\beta}F^{\dagger}_{\boldsymbol{k},\beta\alpha}, \quad (5)$$

where

$$\check{\boldsymbol{H}}_{\boldsymbol{k}} = \begin{pmatrix}\hat{\boldsymbol{M}}_{\boldsymbol{k}} & \hat{\boldsymbol{\Delta}}_{\boldsymbol{k}}, \\ \hat{\boldsymbol{\Delta}}^{\dagger}_{\boldsymbol{k}} & -\hat{\boldsymbol{M}}^{*}_{-\boldsymbol{k}}\end{pmatrix}, \quad (6)$$

with

$$\hat{\boldsymbol{M}}_{\boldsymbol{k}} = \epsilon_k\boldsymbol{\sigma}_0 + \boldsymbol{h}\cdot\boldsymbol{\sigma}. \quad (7)$$

The gap matrix $\hat{\boldsymbol{\Delta}}_{\boldsymbol{k}}$ can be parametrized by introducing a scalar function $\psi_{\boldsymbol{k}}$ with $\psi_{-\boldsymbol{k}} = \psi_{\boldsymbol{k}}$, and further a vector function $\boldsymbol{d}_{\boldsymbol{k}}$ with $\boldsymbol{d}_{-\boldsymbol{k}} = -\boldsymbol{d}_{\boldsymbol{k}}$ (the d-vector). We have

$$\hat{\boldsymbol{\Delta}}_k = \begin{cases}\Delta_s\psi_{\boldsymbol{k}}(\mathrm{i}\sigma_y) & \text{for spin-singlet,}\\ \Delta_t\boldsymbol{d}_k\cdot\boldsymbol{\sigma}(\mathrm{i}\sigma_y) & \text{for spin-triplet,}\end{cases} \quad (8)$$

where the amplitudes Δ_s and Δ_t are chosen to be real and positive.

The pairing potentials in (4) are taken to be

$$V_{\alpha\beta,\lambda\mu}(\boldsymbol{k},\boldsymbol{k}') = -\frac{V_s}{2}(\psi_{\boldsymbol{k}}\mathrm{i}\sigma_y)_{\alpha\beta}(\psi_{\boldsymbol{k}'}\mathrm{i}\sigma_y)^{\dagger}_{\lambda\mu} \quad (9)$$

for spin-singlet states, and

$$V_{\alpha\beta,\lambda\mu}(\boldsymbol{k},\boldsymbol{k}') = -\frac{V_t}{2}(\boldsymbol{d}_{\boldsymbol{k}}\cdot\boldsymbol{\sigma}\mathrm{i}\sigma_y)_{\alpha\beta}(\boldsymbol{d}_{\boldsymbol{k}'}\cdot\boldsymbol{\sigma}\mathrm{i}\sigma_y)^{\dagger}_{\lambda\mu} \quad (10)$$

for spin-triplet states, where V_s, $V_t > 0$.

The excitation spectrum of Bogoliubov-de Gennes quasiparticle $E(\boldsymbol{k})$ can be obtained readily by diagonalizing the matrix $\check{\boldsymbol{H}}_{\boldsymbol{k}}$ in (6). For the ZF oriented in the direction (θ_h, ϕ_h), one can generally find four solutions, namely, $E^{(e)}_{\pm}(\boldsymbol{k})$ and $E^{(h)}_{\pm}(\boldsymbol{k})$, with $E^{(h)}_{\pm}(\boldsymbol{k}) = -E^{(e)}_{\pm}(-\boldsymbol{k})$. The electronic specific heat C_e can be expressed as

$$C_e = \sum_{\boldsymbol{k}}\sum_{\gamma=\pm}E^{(e)}_{\gamma}(\boldsymbol{k})\frac{\partial f_{\boldsymbol{k}\gamma}}{\partial T}, \quad (11)$$

where

$$f_{\boldsymbol{k}\gamma} = f(E^{(e)}_{\gamma}(\boldsymbol{k})) = \frac{1}{\exp(E^{(e)}_{\gamma}(\boldsymbol{k})/T) + 1}. \quad (12)$$

Temperature dependence of the gap amplitude Δ_s or Δ_t is determined by the gap equation

$$\Delta_\alpha = V_\alpha\sum_{k\gamma}\frac{\tanh(E^{(e)}_{\alpha\gamma}(\boldsymbol{k})/2T)}{4}\frac{\partial E^{(e)}_{\alpha\gamma}(\boldsymbol{k})}{\partial\Delta_\alpha}, \quad (13)$$

with $\alpha = s$ or t.

2 Results and discussion

The nodal structure of a superconducting state is determined by zeros of quasiparticle excitation spectra $E^{(e)}_{\pm}(\boldsymbol{k})$ in momentum space. We first consider the spin-singlet case. The quasiparticle excitation spectra of spin-singlet state take a simple form in the presence of ZF,

$$E^{(e)}_{s\pm}(\boldsymbol{k}) = \sqrt{\epsilon_k^2 + \Delta_s^2 + |\psi_{\boldsymbol{k}}|^2} \pm h. \quad (14)$$

As can be seen, $E^{(e)}_{s\pm}(\boldsymbol{k})$ are independent of the orientation of the ZF, an important feature specific to spin-singlet states. It is evident that the upper branch $E^{(e)}_{s+}(\boldsymbol{k})$ has no node, while the lower branch $E^{(e)}_{s-}(\boldsymbol{k})$ may show nodes when

$$\Delta_s|\psi_{\boldsymbol{k}}| \leqslant h. \quad (15)$$

For $h = 0$ this condition becomes

$$|\psi_{\boldsymbol{k}}| = 0. \quad (16)$$

Equations (15) and (16) imply that, for nodal spin-singlet state, new nodes can be induced in the vicinity of the original nodal points or lines by an arbitrarily orientated weak ZF. For example, we consider two typical d-wave states

$$\psi_{\boldsymbol{k}} = \begin{cases}2\hat{k}_z^2 - \hat{k}_x^2 - \hat{k}_y^2 & (d_{2z^2-x^2-y^2}-\text{wave}),\\ (\hat{k}_x^2 - \hat{k}_x^2) + \mathrm{i}\,\hat{k}_x\hat{k}_y & (d_{x^2-y^2}+\mathrm{i}d_{xy}-\text{wave}).\end{cases} \quad (17)$$

The $d_{2z^2-x^2-y^2}$-wave state possesses two isolated line nodes locating at $\theta_k = \arccos\frac{1}{\sqrt{3}}$ and $\theta_k = \pi - \arccos\frac{1}{\sqrt{3}}$ on the Fermi surface. By introducing ZF, these line nodes are spread to two strips [see Fig. 1(a) and 1(b)]. On the other hand, the $d_{x^2-y^2}+\mathrm{i}d_{xy}$-wave state exhibits two isolated second-order point nodes, one at each of the poles on the Fermi surface. These point nodes change to two spots when the ZF is switched on [see Fig. 1(c) and 1(d)]. The width of the strip and the size of the spot are restricted by the condition given in (15).

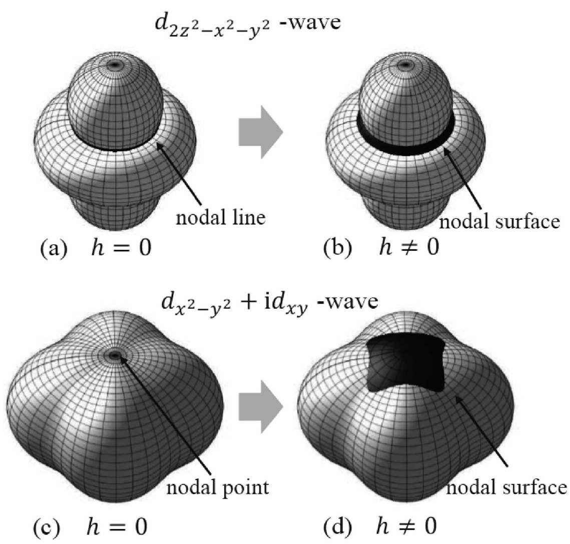

(a) and (b) for $d_{2z^2-x^2-y^2}$-wave; (c) and (d) for $d_{x^2-y^2}+\mathrm{i}d_{xy}$-wave. The black areas denote the induced nodal surfaces.

Fig. 1 Schematic illustration of the evolution of the nodal structure under the influence of ZF

The change in nodal topology will be reflected on the temperature dependence of electronic specific heat at low temperatures. In the absence of ZF, the temperature dependence of specific heat of our two d-wave states follows the standard power-law dependence $C_e(T)\sim T^2$. However, an arbitrarily weak ZF (irrespective of its orientation) can result in change in the exponent, and we have $C_e(T)\sim T$ for $\boldsymbol{h}\neq 0$. In Fig. 2 we present the normalized electronic specific heat $C_e(T)/C_n(T)$ as a function of T/T_c for $d_{2z^2-x^2-y^2}$-wave and $d_{x^2-y^2}+\mathrm{i}d_{xy}$-wave at several values of h, where $C_n(T)$ denotes the specific heat in normal state, and T_c is the critical temperature calculated at $h=0$.

Now let us turn to the spin-triplet case. In this work we will confine ourselves to the so-called unitary phase for which $\boldsymbol{d}_{\boldsymbol{k}}\times\boldsymbol{d}_{\boldsymbol{k}}^{*}=0$ for all $\boldsymbol{k}$. In the presence of ZF, the quasiparticle excitation spectra can be expressed as

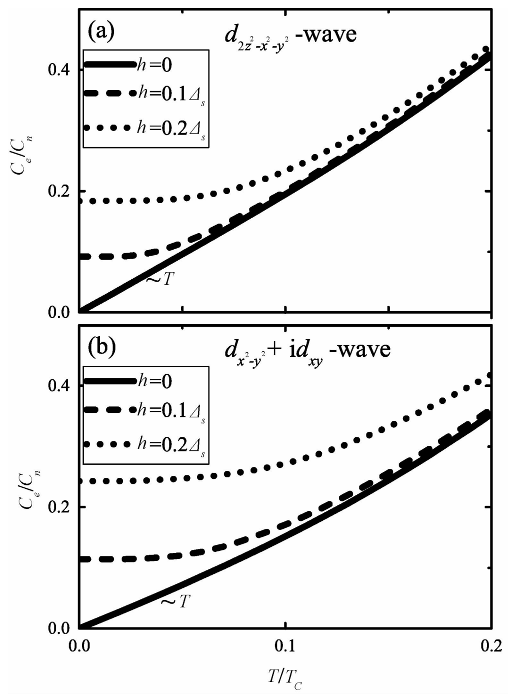

Fig. 2 Temperature dependence of electronic specific heat at low temperatures at several values of h

$$E_{t\pm}^{(e)}(\boldsymbol{k})=\sqrt{\epsilon_k^2+h^2+\Delta_t^2|\boldsymbol{d}_{\boldsymbol{k}}|^2\pm 2S_k}. \quad (18)$$

$$S_{\boldsymbol{k}}=\sqrt{(\epsilon_k^2+\Delta_t^2|\boldsymbol{d}_{\boldsymbol{k}}|^2)h^2-\Delta_t^2|\boldsymbol{d}_{\boldsymbol{k}}\times\boldsymbol{h}|^2}. \quad (19)$$

For $\boldsymbol{h}=0$, $E_{t\pm}^{(e)}(\boldsymbol{k})$ may have nodes at momentum $\boldsymbol{k}$ where $|\boldsymbol{d}_{\boldsymbol{k}}|=0$ on the Fermi surface. However, $E_{t+}^{(e)}(\boldsymbol{k})$ is positive definite in the $\boldsymbol{h}\neq 0$ case. Thereby we only need to discuss the zeros of the lower branch $E_{t-}^{(e)}(\boldsymbol{k})$. Now $E_{t-}^{(e)}(\boldsymbol{k})$ depends on both magnitude and orientation of ZF. Since the Hermitian property of $\check{\boldsymbol{H}}_{\boldsymbol{k}}$ ensures that the eigenvalue $E_{t-}^{(e)}(\boldsymbol{k})$ is real, we get the inequality

$$\epsilon_k^2+h^2+\Delta_t^2|\boldsymbol{d}_{\boldsymbol{k}}|^2-2S_{\boldsymbol{k}}\geqslant 0, \quad (20)$$

which can be rewritten as

$$(\epsilon_k^2-h^2+\Delta_t^2|\boldsymbol{d}_{\boldsymbol{k}}|^2)^2+4\Delta_t^2|\boldsymbol{d}_{\boldsymbol{k}}\times\boldsymbol{h}|^2\geqslant 0. \quad (21)$$

Evidently, $E_{t-}^{(e)}(\boldsymbol{k})=0$ only if the following conditions are satisfied simultaneously:

$$\epsilon_k^2-h^2+\Delta_t^2|\boldsymbol{d}_{\boldsymbol{k}}|^2=0,\ |\boldsymbol{d}_{\boldsymbol{k}}\times\boldsymbol{h}|=0. \quad (22)$$

For $\boldsymbol{h}=0$ these conditions are reduced to

$$|\boldsymbol{d}_{\boldsymbol{k}}|=0. \quad (23)$$

Eq. (22) indicates that, in the presence of ZF, the energy gap in the quasiparticle excitation spectrum closes in the (θ_k,ϕ_k) direction on the Fermi surface, when

$$\Delta_t|\boldsymbol{d}_{\boldsymbol{k}}|\leqslant \boldsymbol{h} \quad (24)$$

for $\boldsymbol{d}_k \times \boldsymbol{h} = 0$, and

$$|\boldsymbol{d}_k| = 0 \quad (25)$$

for $\boldsymbol{d}_k \times \boldsymbol{h} \neq 0$. In the presence of ZF it is convenient to introduce an opposite spin pairing (OSP) state (for which $\boldsymbol{d}_k \times \boldsymbol{h} = 0$ for all $\boldsymbol{k}$) and an equal spin pairing (ESP) state (for which $\boldsymbol{d}_k \cdot \boldsymbol{h} = 0$ for all $\boldsymbol{k}$)[14]. Then the spin-triplet states can be separated into three classes: those that contain only OPS states, those that contain only ESP states, and those that contain both OSP and ESP states. The spin-singlet states can be classified as the OPS states. We note that the condition Eq. (24) for $\boldsymbol{d}_k \times \boldsymbol{h} = 0$ is similar to that of spin-singlet case [Eq. (15)]. This result is reasonable since in such a configuration both spin-singlet and spin-triplet states belong to the OSP states. On the other hand, Eq. (25) states that no additional nodes can be created by ZF at momentum $\boldsymbol{k}$ on the Fermi surface provided that $\boldsymbol{h}$ and $\boldsymbol{d}_k$ are non-collinear, in strong contrast with the spin-singlet case.

Now let us consider two special types of nodal p-wave states for which the d-vectors are independent of the momentum $\boldsymbol{k}$. Here for illustrative purposes we choose the A-phase and Polar-phase in superfluid ^{3}He. The d-vectors[4] can be written as

$$\boldsymbol{d}_k = \begin{cases} \boldsymbol{x}(\hat{k}_x + \mathrm{i}\hat{k}_y), & \text{A-phase}, \\ \boldsymbol{z}\hat{k}_z, & \text{Polar-phase}. \end{cases} \quad (26)$$

The effects of non-magnetic impurity scattering on the thermodynamic quantities in these states were extensively discussed previously[5-8]. At $\boldsymbol{h} = 0$, the A-phase shows the same nodal structure as that of the $d_{x^2-y^2} + \mathrm{i}d_{xy}$-wave state but with the point nodes of first-order, while the Polar-phase possesses line node which is located on the equatorial circle on the Fermi surface. As discussed above, no change in nodal topology would take place for our two phases as long as $\boldsymbol{d}_k \times \boldsymbol{h} \neq 0$. In the $\boldsymbol{h} \parallel \boldsymbol{d}_k$ case, however, they are in the OSP states and the point and line nodes are replaced by nodal surfaces (see Fig. 3), similar to the spin-singlet case discussed above.

We display in Fig. 4 the temperature dependence of electronic specific heat for the A-phase and Polar-phase. In the absence of ZF, the temperature dependence of electronic specific heat for our two phases obey the standard power-law dependence, and we have $C_e(T) \sim T^3$ for A-phase and $C_e(T) \sim T^2$ for Polar-phase. As can be seen, the exponents are unchanged as long as $\boldsymbol{d}_k \times \boldsymbol{h} \neq 0$. For the $\boldsymbol{h} \parallel \boldsymbol{d}_k$ case, however, we obtain $n = 1$ for both phases, as in the case of our spin-singlet states. Note that, when $\boldsymbol{h} \parallel z$ ($\boldsymbol{h} \parallel \boldsymbol{x}$) the A-phase (Polar-phase) is in the ESP state and the $C_e(T)$ varieswith temperature as if $\boldsymbol{h} = 0$.

We proceed to discuss the opposite situation for

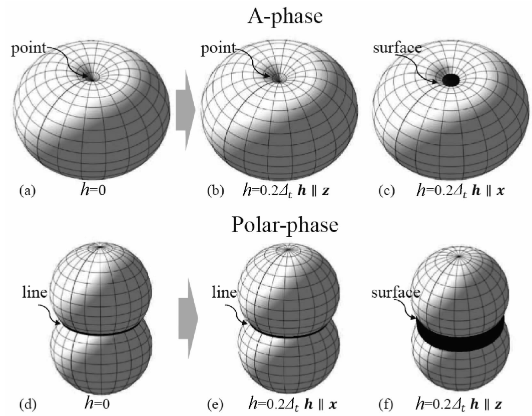

(a) – (c) are for A-phase, and (d) – (f) for Polar-phase

Fig. 3 A surface node created by ZF only when the two vectors $\boldsymbol{h}$ and $\boldsymbol{d}_k$ are collinear

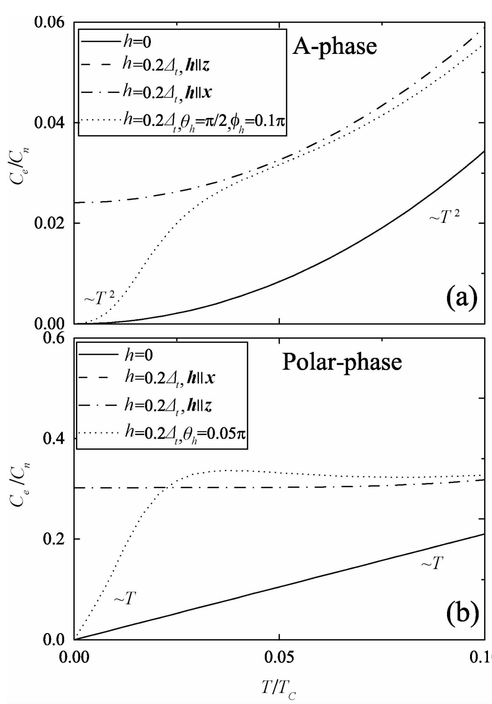

Fig. 4 Calculated temperature dependence of specific heat for A-phase (a) and Polar-phase with different h (b)

which the direction of d-vector is a function of $\boldsymbol{k}$. Here we consider a set of nodal p-wave states[15] given by

$$\boldsymbol{d}_{\boldsymbol{k}} = \begin{cases} \boldsymbol{x}\hat{k}_x \pm \boldsymbol{y}\hat{k}_y, \\ \boldsymbol{x}\hat{k}_y \pm \boldsymbol{y}\hat{k}_x. \end{cases} \tag{27}$$

Note that the d-vectors are confined within the $x-y$ plane. In the absence of ZF, these states exhibit two point nodes of first-order locating at the poles as in the case of A-phase. This nodal structure is unchanged for a ZF not lying in the $x-y$ plane since $\boldsymbol{d}_{\boldsymbol{k}} \times \boldsymbol{h} \neq 0$ in this configuration. When ZF is applied along the $(\theta_h = \pi/2, \phi_h)$ direction, however, the condition given in (24) yields two line nodes across the south and north poles on the Fermi surface, with the size of line node limited by $0 < \theta_k \leqslant \arcsin \dfrac{h}{\Delta_t}$ (see Fig. 5 for $\boldsymbol{d}_{\boldsymbol{k}} = \boldsymbol{x}\hat{k}_y - \boldsymbol{y}\hat{k}_x$ case). The equation which specifies the location of line node across the south pole (i. e. the azimuthal angle ϕ_k) can be obtained from the condition $\boldsymbol{d}_{\boldsymbol{k}} \times \boldsymbol{h} = 0$

$$\begin{cases} \sin(\phi_k \mp \phi_h) = 0 \quad \text{for} \quad \boldsymbol{d}_{\boldsymbol{k}} = \boldsymbol{x}\hat{k}_x \pm \boldsymbol{y}\hat{k}_y, \\ \cos(\phi_k \pm \phi_h) = 0 \quad \text{for} \quad \boldsymbol{d}_{\boldsymbol{k}} = \boldsymbol{x}\hat{k}_y \pm \boldsymbol{y}\hat{k}_x. \end{cases} \tag{28}$$

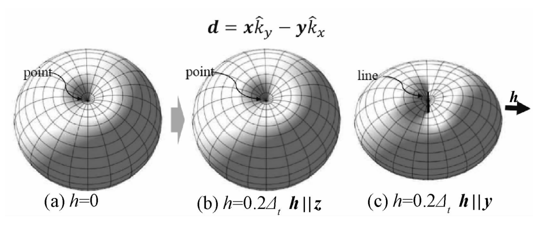

The location of line node depends on the angle ϕ_h.

Fig. 5 Nodal lines for $\boldsymbol{d}_k = \boldsymbol{x}\hat{k}_y - \boldsymbol{y}\hat{k}_x$ state induced only when $\boldsymbol{h}$ is in the $x-y$ plane

Plotted in Fig. 6 is the temperature dependence of electronic specific heat for our states cited above. At $\boldsymbol{h} = 0$, we have $C_e(T) \sim T^3$ as expected. For $\boldsymbol{h} \parallel \boldsymbol{z}$, our states are in the ESP states. Therefore the resultant curve is coincident with that for the $\boldsymbol{h} = 0$ case. This T^3 dependence of $C_e(T)$ is maintained as long as $\theta_h \neq \pi/2$. When $\boldsymbol{h} \parallel \boldsymbol{x}$, the exponent is modified to be $n = 2$ due to the appearance of the induced line nodes mentioned above. It is noted that no quasiparticle excitation exists at $T = 0$ now because of the lack of nodal surface. Finally we discuss in passing the B-phase of superfluid ^{3}He where the d-vector is given by $\boldsymbol{d}_{\boldsymbol{k}} = \boldsymbol{x}\hat{k}_x + \boldsymbol{y}\hat{k}_y + \boldsymbol{z}\hat{k}_z$. In fact this p-wave state is fully gapped. For a ZF applied along (θ_h, ϕ_h) direction, two point nodes are induced at $(\theta_k = \theta_h, \phi_k = \phi_h)$ and $(\theta_k = \pi - \theta_h, \phi_k = \pi + \phi_h)$ on the Fermi surface when $h \geqslant \Delta_t$. In general, no surface nodes is induced if the direction of the d-vector is dependent on $\boldsymbol{k}$.

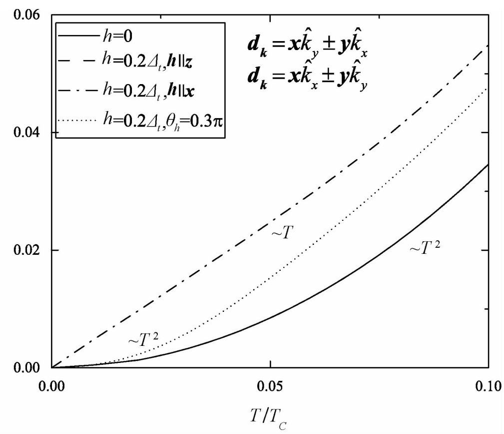

Fig. 6 Calculated temperature dependence of specific heat for $d_k = x\hat{k}_y \pm y\hat{k}_x$ and $d_k = x\hat{k}_x \pm y\hat{k}_y$ states with different h

3 Summary

In summary, we have systematically investigated the effects of a weak ZF on the nodal structures of nodal spin-singlet and nodal unitary spin-triplet superconductors. Detailed analysis of the quasiparticle excitation spectrum indicates that the nodal structure can be changed profoundly under the influence of ZF. This result is corroborated by numerical computations of the low-temperature electronic specific heat $C_e(T)$. We find especially that, for the spin-singlet superconductors or spin-triplet superconductors in the OSP states, a weak ZF may convert the original isolated point or line nodes into surface nodes, which is responsible for the $C_e(T) \sim T$ dependence at low temperatures. In addition, the low-temperature electronic specific heat for spin-triple states is found to be sensitive to the relative orientation between $\boldsymbol{h}$ and $\boldsymbol{d}_{\boldsymbol{k}}$ in a rather peculiar way. We hope that our results would be helpful for identifying the order-parameter symmetry of nodal superconductors.

References

[1] Bennemann K H, Ketterson J B. Superconductivity[M]. Berlin: Springer, 2008.

[2] Kimura N, Bonalde I. Non-centrosymmetric heavy-fermion superconductors [C] // Bauer E, Sigrist M. Non-Centrosymmetric Superconductors. Berlin: Springer, 2012: 35-80.

[3] Volovik G E, Gor'kov L P. Superconducting classes in heavy fermions systems[J]. Zh Eksp Teor Fiz, 1985, 88 (4): 1 412-1 429.

[4] Mineev V P, Samokhin K V. Introduction to unconventional superconductivity[M]. London: Gordon and Breach, 1999.

[5] Gor'kov L P, Kalugin P A. Defects and an unusual superconductivity[J]. Pis'ma Zh Eksp Teor Fiz, 1985, 41 (5): 208-210.

[6] Ueda K, Rice T M. Heavy electron superconductors-some consequences of the p-wave[C] // Kasuya T, Saso T. Theory of Heavy Fermions and Valence Fluctuations. Berlin: Springer, 1985: 267-276.

[7] Pethick C J, Pines D. Transport processes in heavy-fermion superconductors[J]. Phys Rev Lett, 1986, 57 (1): 118-121.

[8] Hirschfeld P J, Wölfle P, Einzel D. Consequences of resonant impurity scattering in anisotropic superconductors: thermal and spin relaxation properties[J]. Phys Rev B, 1988, 37(1): 83-97.

[9] Eremin I, Annett J F. Magnetic field dependence of the superconducting gap node topology in noncentrosymmetric $CePt_3Si$[J]. Phys Rev B, 2006, 74 (18): 184524-1-184524-5.

[10] Fujimoto S. Theory of parity-violated Cooper pairs in weakly noncentrosymmetric superconductors[J]. Phys Rev B, 2007, 76(18): 184504-1-184504-7.

[11] Chen C, Jin B. Zeeman field-induced nodal structures in rashba-type noncentrosymmetric superconductors[J]. J Low Temp Phys, 2016, 182(3/4): 124-138.

[12] Hayashi N, Wakabayashi K, Frigeri P A, et al. Temperature dependence of the superfluid density in a noncentrosymmetric superconductor[J]. Phys Rev B, 2006, 73(2): 024504-1-024504-9.

[13] Hayashi N, Wakabayashi K, Frigeri P A, et al. Nuclear magnetic relaxation rate in a noncentrosymmetric superconductor[J]. Phys Rev B, 2006, 73 (9): 092508-1-092508-4.

[14] Powell B J, Annett J F, Györffy B L. The gap equations for spin singlet and triplet ferromagnetic superconductors[J]. J Phys A Math Gen, 2003, 36 (35): 9 289-9 302.

[15] Sigrist M, Ueda K. Phenomenological theory of unconventional superconductivity[J]. Rev Mod Phys, 1991, 63 (2): 239-311.